Correlated host movements can reshape spatio-temporal disease dynamics: modeling the contributions of space use to transmission risk using animal movement data

Juan S. Vargas Soto, Lisa I. Muller, Dan Grove, Justin Kosiewska, Dailee Metts, and Mark Q. Wilber

School of Natural Resources, University of Tennessee, Knoxville, TN

Target Journal: Methods in Ecology and Evolution

Abstract

Understanding how animal movement influences disease transmission processes is critical to manage disease in wildlife and to eventually predict outbreaks or spillovers. These goals, however, require a thorough understanding of the intricate relationships between the environment, movement, and interactions among individuals. Here, we derive and test a framework to estimate a spatially explicit, pairwise, expected risk of disease transmission based on animal movement data (e.g. GPS tracking data). We derive some general conclusions related to direct transmission analytically, test the influence of epidemilogical covariates such as parasite decay rate and contact distance on the estimated FOI Our simulations show that temporal correlation in local space use, which arises from social interactions, can significantly increase the estimated force of infection. This effect was greater for parasites with short environmental persistence (relative to host movement rate). For parasites that persisted for longer in the environment correlation had much smaller influence. Our results provide guidelines that relate the biology of parasites and the inferences that can be made regarding transmission using UDs. Our approach can be easily integrated with frameworks that estimate utilization distributions accounting for environmental covariates, which would allow to create an environmentally-informed FOI that could potentially be extrapolated to other populations and locations. Understanding the environmental and social processes that generate correlations in space use will be key

moving forward to accurately estimate an FOI expected given environmental drivers.

Introduction

Individual movement is among the most critical factors that determine the dynamics of infectious disease in wildlife (Dougherty et al., 2018; Manlove et al., 2022). From an individual perspective, how an animal moves determines whether they encounter other individuals of the same species, other species, or parasites in the environment (Martinez-Garcia et al., 2020; Das et al., 2023). These encounters are a necessary component for the transmission of parasites and infectious diseases, and efforts have sought to identify where they could occur, how often, and how they could be influenced by environmental drivers (Titcomb et al., 2021; Dougherty et al., 2022). Being able to formally link environmental factors, animal movement, contact, and parasite transmission risk, could improve our ability to predict and prevent outbreaks and would represent a significant advancement for management of wildlife diseases. Nevertheless, understanding and extrapolating the relationships between these processes at an individual scale requires extremely detailed information about movement, combined with analytical frameworks that can translate this information into an epidemiological context.

Recent approaches developed at the interface of movement and disease ecology are able to leverage animal tracking data with high spatial and temporal resolution to gain insight into contact among individuals and disease transmission (Richardson and Gorochowski, 2015; Wilber et al., 2022; Yang et al., 2023). For example, movement-driven modeling of spatio-temporal infection risk (MoveSTIR) builds dynamic spatio-temporal contact networks from which we can estimate the risk of infection for different individuals across space and time (Wilber et al., 2022). MoveSTIR provides a theoretical foundation to translate contacts observed or inferred from spatial data into the epidemiological currency of force of infection, which represents the risk of transmission experienced by a host per unit time. These studies have highlighted the importance of individual heterogeneity and temporal scale for disease dynamics, particularly how indirect contact—two individuals at the same place at different times—can significantly reshape contact and transmission networks (Richardson and Gorochowski, 2015; Yang et al., 2023). These approaches are nonetheless based on occurrence, rather than range, distributions (in the terminology of Alston et al., 2022) – meaning it only considers where animals were observed and not where they *potentially* could have moved. This makes it difficult to systematically link observed encounters with underlying spatial covariates, and to predict how social or environmental changes affect contact and transmission.

An alternative approach would be to use utilization distributions (UDs) to infer spatial and temporal contact and transmission probabilistically. An individual's UD is defined as the probability—either transient

or in the long-run (Tao et al., 2016)—that it uses a particular area on a landscape (Worton, 1989), and is perhaps the best representation of the long-term relationship between environment and use of space over different time scales Webber et al. (2023). The high spatial and temporal resolution of modern tracking data serves to build UDs based on biologically realistic movement models (Kranstauber et al., 2012; Fleming et al., 2014), and to link them with underlying resources (Potts and Börger, 2023). Individually defined UDs can be combined to study pairwise interactions, for example to quantify the degree of overlap between home ranges (Winner et al., 2018), or to estimate the expected location and rate of encounter between individuals (Noonan et al., 2021), which could be used to infer contact and transmission (Godfrey et al., 2010; Godfrey, 2013; Noonan et al., 2021). Moreover, because UDs can be directly linked to environmental drivers of movement (Signer et al., 2017), they have the potential to predict contact and transmission in novel environments and can also be used for prospective analyses to understand how the effects of environmental and social perturbations cascade across scales, from individual movement to population and landscape-level disease transmission.

Current contact metrics based on UDs focus only on direct interaction, ignoring temporal dynamics that are especially relevant for epidemiological processes. The Conditional Distribution of Encounters (CDE) (Noonan et al., 2021), for example, estimates the probability that two individuals will come into contact with each other at a given location, assuming that individuals move independently from each other. While a useful simplification, social interactions like territoriality or gregariousness can invalidate this assumption (Manlove et al., 2018; Sah et al., 2018). In these cases, temporal correlations in space use could increase or decrease the expected probability of encounter compared to an assumption of independent movement (Kjær et al., 2008; Schauber et al., 2015). Moreover, direct interactions do not necessarily equate to *epidemiological contacts*, which consist of contact formation, contact duration, pathogen acquisition, pathogen shedding, and pathogen decay. As some parasites can persist in the environment for months or years (e.g. anthrax, CWD), ignoring these processes could severely underestimate the risk of transmission (Wilber et al., 2022; Yang et al., 2023; Richardson and Gorochowski, 2015).

In general, we lack a way to quantify the role of social interactions on spatio-temporal force of infection, which limits our ability to assess when ignoring correlated movements actually matters when assessing infection risk. One of our goals in this study is to ask: how much can correlated, social movements affect spatio-temporal infection risk for directly and indirectly transmitted pathogens? A large portion of epidemiological theory is built upon the assumption of independent host movements in the presence or absence of spatial heterogeneity, but there is very little theory that quantifies how correlated movements affect contact and transmission risk. In contrast, there is a large body of empirical work that empirically quantifies how correlated and social movements can reshape contact and transmission landscapes (Kjær et al., 2008; Grear

et al., 2010; Schauber et al., 2015; Webber et al., 2023) [other citations from non-deer systems needed]. Bridging this gap from what we observe empirically to what we expect theoretically is a key missing link. While the previously developed MoveSTIR implicitly accounts for such correlations, it only applies for observed data. In contrast, the CDE provides a basis for estimating encounter probabilities across the landscape, but ignores correlations and temporal dynamics of indirect contact. Ultimately, an approach is needed that combines the range-distribution inference of UDs and CDEs (Alston et al., 2022; Noonan et al., 2021) with the epidemiological focus of MoveSTIR to link UDs to epidemiological dynamics.

Here, we develop a model we refer to as Probabilistic MoveSTIR (PMoveSTIR) to estimate epidemiological contact and expected force of infection across space and time from UDs. Our approach provides probabilistic, spatio-temporal contact networks that can be used to predict out-of-sample transmission risk. We first derive the most general PMoveSTIR model using transient UDs and then provide different modifications to consider heterogeneities in space and time. We show how PMoveSTIR encompasses other common assumptions such as mass action transmission and home range overlap transmission as special cases. Deriving analytical results and applying PMoveSTIR to simulated movement data, we demonstrate the sometimes sizable importance of non-independent movements on pairwise transmission risk, indicating that ignoring the social drivers of contact could severely bias epidemiological inference. However, our simulations show that this result primarily holds for parasites with short environmental persistence (relative to host movement rate). For parasites that persist for long periods of time in the environment, non-independent host movements are largely inconsequential compared to spatial overlap for transmission risk. We demonstrate this result empirically using a dataset of white-tail deer movements and show that empirically observed correlated movements can increase potential force of infection by orders of magnitude for a hypothetical directly transmitted parasite but are relatively unimportant for a hypothetical parasite with long persistence times. Overall, PMoveSTIR is a critical next step for developing predictive models that link movement data to spatio-temporal infection dynamics on real landscapes.

Methods

Model development - Linking utilization distributions to transmission through PMoveSTIR

PMoveSTIR builds on the recently developed MoveSTIR model (Wilber et al., 2022) and formally links host utilization distributions, direct and indirect contacts, correlated animal movements, and spatial estimates of force of infection (FOI). This an essential quantity in disease ecology that underlies our ability to predict

the spread of disease across populations and landscapes. Essentially, we want to know, for two individuals i and j moving and interacting across a landscape, what is the FOI host i experiences from host j, across space and time?

As in MoveSTIR, we assume that transmission happens by an infected host depositing pathogen into the environment and another host picking that pathogen up. Deposition and acquisition can represent a range of processes, from one individual coughing and another inhaling in a matter of seconds, to one host depositing parasite eggs or larvae in the environment and another individual consuming these days or weeks later. This fairly general assumption encompasses standard density-dependent transmission as a special case (Cortez and Duffy, 2021). Moreover, considering transmission through deposition and acquisition components clearly links direct transmission and indirect transmission along a continuum (Wilber et al., 2022).

In PMoveSTIR, we assume a "contact" can occur if both individuals visit a given location x, which could be a habitat patch or a grid cell. For the results we discuss in the main text, we assume that locations x on the landscape do not overlap such that summing the areas of locations x equals some total area over which individuals can move (in Appendix 1 we provide a derivation when x is a point, not an area, on the landscape). Furthermore, we assume that the likelihood of contact is uniform within the location x, consistent with a so-called top-hat encounter function (Gurarie and Ovaskainen, 2013; Wilber et al., 2022).

Given these assumptions, we can define the pairwise force of infection felt by host i from host j in location x at time t as (Wilber et al., 2022)

$$h_{i \leftarrow j}(t, x) = \int_{-\infty}^{t} \beta' \lambda \delta_{x_j(u)}(x) \delta_{I_j(u)}(I) S(t-u) du \tag{1}$$

where λ is the pathogen deposition rate of host j, $\delta_{x_j(u)}(x)$ is an indicator variable that is one if host j is in location x at time u and zero otherwise, $\delta_{I_j(u)}(I)$ is an indicator function that is one if host j is in an infected state at time u and zero otherwise, and $S(t-u)$ is the probability that any pathogen deposited at time $u < t$ is still alive at time t (see Wilber et al., 2022, for a full derivation). The term β' is the rate at which host i picks up pathogen within the location x and can be re-written as $\tilde{\beta}/A_x$, where $\tilde{\beta}$ can be considered a "search efficiency" term, with units area/time (e.g., m^2/day), and A_x gives the area of location x (e.g., 100 m^2). Therefore, the total acquisition rate scales with the area in which contact can occur; in larger areas, the acquiring host would have to search for longer to find a "packet" of pathogen, reducing the host's total acquisition rate and the corresponding FOI. Moving forward, we assume that host j (the depositing host) is always infected. This is equivalent to building a contact network and also represents the structural form of FOI needed to compute pathogen invasion thresholds (Wilber et al., 2022).

Considering probabilistic movements (i.e., we only know where an individual is with some probability at

a given time), we can then re-write equation 1 as

$$h_{i\leftarrow j}(t,x) = \int_{-\infty}^{t} \beta' \lambda \delta'_{x_i(t)}(x)\delta'_{x_j(u)}(x)S(t-u)du \tag{2}$$

where $\delta'_{x_i(t)}(x)$ and $\delta'_{x_j(u)}(x)$ are random variables that specify whether or not (i.e., 0 or 1) host i or host j is in location x at time t. This means that $h_{i\leftarrow j}(t,x)$ is also a random variable, and we can express its expected value as

$$E[h_{i\leftarrow j}(t,x)] := h^*_{i\leftarrow j}(t,x) = \int_{-\infty}^{t} \beta' \lambda E[\delta'_{x_i(t)}(x)\delta'_{x_j(u)}(x)]S(t-u)du. \tag{3}$$

Interpreting this expectation, we are asking: if we simulated some movement process thousands of times, what is the probability that host i is in location x at time t and host j was in location x at a previous time u?

Linking equation 3 to utilization distributions

Note that for two random variables Y and Z, $E[YZ] = E[Y]E[Z] + Cov(Y,Z)$. We can therefore write equation 3 as

$$\begin{aligned} h^*_{i\leftarrow j}(t,x) &= \int_{-\infty}^{t} \frac{\tilde{\beta}}{A_x} \lambda E[\delta'_{x_i(t)}(x)\delta'_{x_j(u)}(x)]S(t-u)du \\ &= \frac{\tilde{\beta}}{A_x}\lambda \int_{-\infty}^{t} [E[\delta'_{x_i(t)}(x)]E[\delta'_{x_j(u)}(x)] + Cov(\delta'_{x_i(t)}(x), \delta'_{x_j(u)}(x))]S(t-u)du \\ &= \frac{\tilde{\beta}}{A_x}\lambda \int_{-\infty}^{t} [p_i(x,t)p_j(x,u) + Cov(\delta'_{x_i(t)}(x), \delta'_{x_j(u)}(x))]S(t-u)du \end{aligned} \tag{4}$$

where we use the fact that the expectation of an indicator variable is a probability (Grimmett and Stirzaker, 2001). The terms $p_i(x,t)$ and $p_j(x,u)$ give the probabilities that host i and j are in location x at times t and u, respectively, and can also be written as $p_i(x,t) = \int_{A_x} f_i(s,t)ds$ where $f_i(s,t)$ is the probability density of host i using the point s at time t and the integral is over the area A_x (defined equivalently for host j). Thus, we have obtained an equation that links the transient utilization distributions $f_i(s,t)$ and $f_j(s,u)$ with the spatio-temporal FOI.

Applying the PMoveSTIR framework under different degrees of spatial and temporal heterogeneity

Equation 4 is the most general formulation of PMoveSTIR, where utilization distributions and between-individual spatial covariance are time-varying and heterogeneous in space. For example, this could account

for daily changes in habitat use and social interactions. The approach can be modified to consider different degrees of spatial and temporal heterogeneity. This allows us to link FOI to different metrics such as temporally varying utilization distributions, stationary utilization distributions, and home range overlap.

Fig. 1 shows the different scenarios that PMoveSTIR can consider. In the upper-left corner, we consider space use is uniform, but movement is non-stationary. In this case, it is not important where an individual is, just when. Considering this framing from an empirical point of view, proximity loggers deployed on individual hosts — a commonly used tool to measure among-animal contacts (Drewe et al., 2012) — only tell us when contacts between individuals occur, but not where. Thus, we cannot make inference about spatial factors driving contacts, but can make inference on temporal processes. We consider this case in a future study.

In the lower left-hand corner of Fig. 1, we have the case where space use is uniform and time is stationary. For simplicity, we also assume that pathogen decay is exponentially distributed with a rate of decay ν such that $S(s) = \exp(-\nu s)$. Given these assumptions, we can write the FOI equation as

$$h^*_{i \leftarrow j}(A_x) = \beta' \lambda \left[\frac{A_x}{A_{tot}} \frac{A_x}{A_{tot}} \frac{1}{\nu} + \int_0^\infty Cov(\delta_{i \in A_x}, \delta_{j \in A_x} | s) e^{-\nu s} ds \right] \tag{5}$$

where the covariance in contact is constant across all areas A_x on the landscape (such that $\delta_{i \in A_x}$ indicates the use of some arbitrary area A_x). If hosts are moving independently (i.e., covariance is 0) we obtain $\frac{\tilde{\beta}}{A_x} \frac{A_x}{A_{tot}} \frac{A_x}{A_{tot}} \frac{\lambda}{\nu}$. Given a gridded landscape with non-overlapping grids and x is a single grid cell, summing over all n areas A_x that comprise the landscape yields $\bar{h}_{i \leftarrow j} = \frac{\tilde{\beta}}{A_{\text{tot}}} \frac{\lambda}{\nu}$, which is the standard mass action assumption of transmission (McCallum, 2001).

Finally, the lower-right corner represents the special case of statistical stationarity in movement (i.e., the mean location is constant through time, though the animal is still moving). Again assuming that pathogen survival in the environment follows $S(s) = e^{-\nu(s)}$, where ν is a constant pathogen decay rate, we can simplify equation 4 to (derivation in Appendix 2)

$$h^*_{i \leftarrow j}(x) = \frac{\tilde{\beta}}{A_x} \lambda \left[p_i(x) p_j(x) \frac{1}{\nu} + \int_0^\infty Cov(\delta_{i \in x}, \delta_{j \in x} | s) e^{-\nu s} ds \right] \tag{6}$$

The key insight here is that, given a stationarity assumption, the expected force of infection in location x depends on i) the marginal probabilities that host i and host j use location x (i.e. their UDs), and ii) the covariance in how host i and host j use location x, integrated over different time lags s. The UD product is proportional to the probability of encounter between two individuals when their movement is independent (Noonan et al., 2021). To improve intuition, we can redefine $Cov(\delta_{i \in x}, \delta_{j \in x} | s) = \sigma_i(x) \sigma_j(x) Cor(\delta_{i \in x}, \delta_{j \in x} | s)$,

where $\sigma_i(x) = \sqrt{p_i(x)(1-p_i(x))}$ and $\sigma_j(x) = \sqrt{p_j(x)(1-p_j(x))}$ are the standard deviation in probability of host i and j using location x, respectively. We can then write

$$h^*_{i \leftarrow j}(x) = \beta' \lambda [\underbrace{p_i(x)p_j(x)\frac{1}{\nu}}_{\substack{\text{FOI contribution from} \\ \text{shared space use}}} + \sigma_i(x)\sigma_j(x) \underbrace{\int_0^\infty Cor(\delta_{i \in x}, \delta_{j \in x} | s) e^{-\nu s} ds}_{\substack{\text{FOI contribution from} \\ \text{correlated movement}}}] . \quad (7)$$

In equations 6 and 7, the $1/\nu$ term represents the scaling due to the parasite decay, assuming we are integrating over infinite lags. In practice we will actually have a limited time given by the data, which sets an upper limit on the lags that can be considered. If this time is short relative to the parasite decay function there could be substantial error in the estimation. A more formal approach is then to use the integral over a specific period $\int_0^\tau e^{-\nu s} ds = (1 - e^{-\nu \tau})/\nu$. Equation 7 highlights that the key quantity we need to understand is the correlation in host i's and host j's use of location x at different time lags s, i.e. the temporal cross-correlation in space use. This correlation is most easily understood for short time lags ($s \approx 0$), for which a positive value indicates that individuals are at the same location at the same time or one shortly after the other. In contrast, negative correlations at short lags indicate the individuals rarely encounter each other directly. In what follows, we focus on this case and explore how and under what circumstances correlated movement can influence the FOI. We analyze different scenarios of movement analytically, using simulations, as well as empirical data. In Appendix X, we examine two additional formulations of PMoveSTIR that highlight the flexibility of this approach for linking range distributions (including home ranges and UDs) and spatial-temporal infection risk.

Analytical and simulation insight into correlated movement and FOI

Leveraging PMoveSTIR, we used analytical analysis, simulation, and empirical data to ask: how much can correlated, social movements affect spatio-temporal infection risk for directly and indirectly transmitted parasites? First, we used PMoveSTIR to derive a general formula that explicitly quantifies how much correlation can augment or reduce force of infection due to direct contact compared to random movement. We also derived analytical results for a specific movement pattern to demonstrate how correlated movements alter transmission risk due to indirect transmission. Second, we used simulations to explore how temporally correlated movements affect transmission, and how the pairwise FOI estimate depends on epidemiological parameters such as contact distance and parasite survival. In eq.6, the correlation component is entirely dependent on the observed trajectories and is therefore susceptible to the amount of data available. We explored the implications of this by simulating different tracking times. We focus on the lower-right corner of the PMoveSTIR box (eq. 7), where we assume statistical stationarity in movement. The process for

calculating the FOI across the landscape is summarized in Fig. 2.

In every simulation, we have two individuals moving around established home ranges, according to an Ornstein-Uhlenbeck process. To create different levels of correlation, we modify the initial simulated tracks using a convolution approach with a social interaction kernel (Scharf et al., 2018). This method accounts for constant or temporally varying attraction between pairs of individuals. For our purposes we assume attraction strength is constant in time, but varies across pairs from 0 (completely independent movement) to 1 (joint movement). Strong interactions lead to similar and highly overlapping trajectories, which could represent animals in a herd, courting/mating pairs, or parents with their offspring. For every scenario, we fit continuous-time movement models to the simulated tracks, and estimate individual UDs using autocorrelated kernel density estimation (Calabrese et al., 2016). We estimate the UDs on a grid of square cells, where the cell side d is the threshold contact distance for epidemiological contact.

We use the UDs to calculate the product of the probabilities of use ($p_i(x)p_j(x)$) and the product of their standard deviations ($\sqrt{p_i(x)(1-p_i(x))}\sqrt{p_j(x)(1-p_j(x))}$) for each grid cell. Both products are symmetrical for every pair of individuals. The lagged correlation term is calculated based on the position history for each individual at locations that both visited (locations that only one or neither individual visited have a correlation of zero). This is a binary vector that specifies whether each individual was present (1) or absent (0) at location x at time t. The order of visits matters, so these correlation values can be asymmetric between individuals. Correlations can appear spuriously even in the absence of a true interaction, particularly for time series, which are often autocorrelated. To address this issue, we performed a prewhitening step to remove the potential effects of autocorrelation on the estimated cross-correlation. This procedure consists of fitting an autoregression model to one of the series, and filtering both of them using the coefficients estimated from the model (Dean and Dunsmuir, 2016). Additionally, we retained only correlation values that were significantly different from 0, i.e. correlations with absolute values greater than a threshold of $1.96/\sqrt{(N)}$, where N is the length of each time series (Dean and Dunsmuir, 2016). All other values were set to 0 as they are considered random noise. We then scale each correlation value by $e^{-\nu s}$ due to the decay of the parasite, where s is the lag corresponding to each cross-correlation, between 0 and $t - dt$, and dt is the (constant) time lag between observations.

Substituting the terms in equation 7 and scaling by the epidemiological parameters $\tilde{\beta}\lambda/A_x$ we obtain the per-cell FOI. Negative correlation terms could occasionally make a cell's estimated FOI negative, especially for small cells where the probabilities of use are low; the FOI is nevertheless strictly positive by definition, so in these cases we set the cell FOI to zero. Through these simulations we explore how the expected FOI is influenced by correlation in space use, home range overlap, parasite decay rate, and contact distance.

Empirical application - White-tailed deer

To test the role of space-use and correlated movements on potential transmission risk in a real system, we applied the PMoveSTIR model to GPS-tracking data for five white-tailed deer (*Odocoileus virginianus*) from Ames Plantation, Tennessee, USA (two bucks and three does). Deer were captured and equipped with GPS collars that recorded fixes every 30 minutes (Lotek LifeTrack IR 420; IACUC # 2850-1021 from the University of Tennessee). All individuals used in this study were captured at the end of March 2023 but we only included movement data from May to June in this study (removing April data to eliminate any capture effects on movement). We fit continuous-time movement models to each track and estimated the utilization distributions (UD) using AKDEs (Calabrese et al., 2016). Using the fitted continuous-time movement model for each individual, we interpolated the positions to regular 10 minute intervals to account for missed fixes (Yang et al., 2023). We defined a contact as occurring when hosts occupied the same 10m by 10m square cell.

We modeled two hypothetical pathogens. The first pathogen had a relatively short persistence time in the environment, surviving for an average of 1 hour ($\nu = 1h^{-1}$). In this case, transmission is largely direct and this might represent a pathogen like SARS-COV-2, which can infect and transmit between white-tailed deer (Hale et al., 2022). The second hypothetical pathogen had a long persistence time, remaining viable for over a year on average ($\nu = 0.9yr^{-1}$). In this case, transmission is largely indirect and might reflect a pathogen like chronic wasting disease (CWD), which can transmit directly and indirectly between deer and can persist for years in the environment (Saunders et al., 2012). The β and λ parameters are scalars in PMoveSTIR and do not affect any relative comparisons, so we set them both to unity. As in the simulations, we prewhitened and filtered correlation values to remove potentially spurious correlations. We use these data to explore how differences in overlap across home ranges and correlated movement influence the expected FOI with real animal trajectories.

Results

The importance of correlated movements on FOI – analytical results

To gain analytical intuition into the role that correlated movement can have on FOI, consider equation 5 where movement is statistically stationary and hosts use space uniformly. As we showed above, when correlation in movement is zero, equation 5 reduces to mass action transmission. For illustrative purposes, consider a case where two individual hosts are moving together across some area A_{tot}. We assume that hosts spend η time units within a habitat patch/grid cell of area A_x before moving to the next patch/grid cell.

Second, we assume that the pathogen survival function $S(s)$ is a step function with a survival probability of one when lag $s \leq \pi\eta$ and zero when $s > \pi\eta$. The term $\pi\eta$ gives the time the pathogen survives in the environment as a function of host residence time, where π ranges from near zero for directly transmitted pathogens to some arbitrarily large number for pathogens with long environmental persistence times. In this scenario, transmission can only occur while both animals are in the same patch. With these assumptions, we can rewrite equation 5 as

$$h^*_{i \leftarrow j}(A_x) = \beta' \lambda \left[\frac{A_x}{A_{tot}} \frac{A_x}{A_{tot}} \pi\eta + \frac{A_x}{A_{tot}} (1 - \frac{A_x}{A_{tot}}) \int_0^{\pi\eta} Cor(\delta_{i \in A_x}, \delta_{j \in A_x} | s) ds \right], \tag{8}$$

recognizing that $\sigma_i(x)\sigma_j(x) = \sqrt{\frac{A_x}{A_{tot}}(1 - \frac{A_x}{A_{tot}})} \sqrt{\frac{A_x}{A_{tot}}(1 - \frac{A_x}{A_{tot}})} = \frac{A_x}{A_{tot}}(1 - \frac{A_x}{A_{tot}})$ when both hosts are using space uniformly.

Direct transmission

For hosts that are moving together, $Cor(\delta_{i \in A_x}, \delta_{j \in A_x} | s)$ will be exactly unity when lag $s = 0$ and near unity when lag s is near zero. When pathogens are strictly directly transmitted, π is also small and if $\pi\eta << \eta$ then we can reasonably approximate $Cor(\delta_{i \in A_x}, \delta_{j \in A_x} | s) = 1$ for s from 0 to $\pi\eta$. We can then write equation 8 as

$$h^*_{i \leftarrow j}(A_x) = \beta' \lambda \pi\eta \left[\underbrace{\frac{A_x}{A_{tot}} \frac{A_x}{A_{tot}}}_{\substack{\text{Contribution due} \\ \text{to habitat overlap}}} + \underbrace{\frac{A_x}{A_{tot}} (1 - \frac{A_x}{A_{tot}})}_{\substack{\text{Contribution due} \\ \text{to correlated movement}}} \right]. \tag{9}$$

The relative contribution of correlation in movement with respect to the contribution due to habitat overlap is simply $(1 - (A_x/A_{tot}))/(A_x/A_{tot}) = A_{tot}/A_x - 1$. Thus, PMoveSTIR allows us to put intuitive bounds on the importance of correlated movements for direct transmission risk. As the area A_x in which an epidemiological contact can occur gets smaller relative to the total area in which the hosts are moving A_{tot}, the correlated movement can have an orders of magnitude larger contribution to direct transmission FOI than habitat overlap at the scale of the area A_x (Fig. 3). If there are large correlations across multiple areas this will add up into a significantly greater FOI across the entire landscape. This makes intuitive sense. If the area of potential contact is small and hosts are moving randomly, there is a very low chance that hosts will be there together at the same time. Having highly correlated movements significantly increases the chance that hosts are in this relatively small area at the same time. Importantly, our results show that even when correlation between animal movements is low (e.g. 0.1), the contribution of correlation to FOI can still be 10 times

greater than spatial overlap if the area of contact is small (e.g., $< 5\%$ of the total area; Fig. 3).

In contrast, when the area of contact A_x approaches A_{tot} (or more generally when the probability of using a particular area is very high), the importance of correlated movement relative to habitat overlap becomes minimal (Fig. 3). For example, if two hosts are always using a particular contact area together because of high resource availability, then it does not matter for FOI if social factors are leading to additional correlated movement. This result extends beyond epidemiological contexts and shows when correlated movements can significantly alter contact risk based on metrics such as home range overlap or CDE.

Indirect transmission

The effects of correlated movement on FOI relative to habitat overlap become analytically more difficult to generalize when we consider pathogens with indirect transmission. This is because the correlation function $Cor(\delta_{i\in A_x}, \delta_{j\in A_x}|s)$ can be highly non-trivial even in the simple case when two hosts are moving together. For example, even individuals that never encounter each other directly can have positive correlations at relatively short lags, and these can be greater than the correlations for individuals that do come into direct contact but only overlap partially at the same locations (Fig. S1b,c). While determining the analytical form of $Cor(\delta_{i\in A_x}, \delta_{j\in A_x}|s)$ for common movement models is beyond the scope of this study, we can use a relatively simple movement scenario to get an analytical sense of how indirect transmission and correlated movements can interact to affect transmission risk. We provide the analytical example in Appendix S3. The example illustrates three important points: 1) the contributions of correlated movement to indirect transmission risk will depend strongly on the movement dynamics as reflected in $Cor(\delta_{i\in A_x}, \delta_{j\in A_x}|s)$; 2) this contribution could potentially increase, decrease, or have no effect on local FOI depending on the lag considered; 3) the relative importance of correlations at different lags is determined by the parasite survival function. Below, we explore these factors using simulations.

Simulation study

Effect of correlated movement on pairwise FOI

Generally, greater interaction strengths led to higher overlap among home ranges. Simulations with interaction strengths greater than 0.9 all resulted in overlap values greater than 0.99, meaning the utilization distributions were always virtually identical. Pairs moving independently had lower overlap values on average but also higher variance, so some pairs had similarly high overlap (>0.9). This allows us to compare the FOI while teasing apart the effects of spatial overlap and temporal correlation in space use.

The FOI was higher for pairs with higher interaction strengths, i.e. pairs that were more attracted to

each other. This increase was due in part to higher spatial overlap, as can be seen from the higher FOI values calculated using only the stationary utilization distribution component (Fig. 4a). However, we saw a greater increase in FOI when we accounted for temporal correlation, and the difference between the two increased with higher interaction strengths. For very similar trajectories (interaction > 0.9), the FOI with correlation was more than ten times the FOI estimated without correlation, and there was a more than 100-fold difference for perfectly overlapping trajectories. Methods that ignore temporal correlation could therefore be significantly underestimating transmission risk.

Accounting for correlation usually resulted in an increase in the estimated FOI; in only 19% of cases the estimates were equal with or without correlation, and in no instance was there a decrease. This is to be expected as we only included attraction, and not avoidance, in the simulations. We found that correlation could increase the estimated FOI even for pairs that moved independently. In 75% of these simulations there was virtually no difference in FOI estimates with and without correlation, and 86% saw less than 20% increase. There were nonetheless instances where the estimated overall FOI was significantly greater, more than three times greater in some cases where the individuals had a high degree of home range overlap (Fig. 4d). For pairs with low overlap, on the other hand, correlation usually did not play a significant role. While the expected correlation is 0 when individuals are known to be moving independently, the joint use of space could lead to an apparent correlation in the observed data, especially when there are few observations in a given cell. This is important to keep in mind when analyzing empirical data where the true correlation nor the degree of attraction/avoidance among individuals is known.

Influence of data availability

The length of the data series had a significant influence on estimated FOI. With longer time series, the number of cells that both animals in a pair visited, and for which correlation is calculated, increased linearly. However, the proportion of those cells where the FOI estimates were different with and without the correlation component actually decreased. This could be interpreted as a decrease in the estimated correlations as more visits are made to the same cells. While the proportion of cells that effectively modify the FOI estimated from spatial overlap decreases, the absolute number of these cells is still greater, and the overall effect is an increased FOI when there are longer time series. In our simulations, there are no underlying environmental covariates driving movement or correlation in space use, so the expected correlation is uniform across the landscape. The cumulative correlation, however, is not related to the product of the UDs or the product of the standard deviations. Getting more data means that the correlations at the local (cell) level become more accurate, and that the correlation can be estimated for more locations. Empirical movement studies should therefore try to ensure that the tracking duration is sufficient for the animals to cover the majority of their

home range, so that estimated correlations are representative of the true underlying relationship. Given the complexity of the correlation, which may be determined through a combination of environmental factors and specific social interactions, predicting the underlying correlation surface could prove quite challenging.

Influence of epidemiological parameters

We also analyzed how changes in epidemiological parameters, namely the parasite decay rate and the contact distance, influenced the estimated risk of transmission. The FOI was inversely proportional to decay rate; if parasites survived longer in the environment this led to higher estimated FOI (Fig. 4b). This increase is driven mostly by the linear increase in the spatial overlap component ($p_i(x)p_j(x)/\nu$), for longer decay times the relative contribution of the correlation term to the estimated FOI decreased significantly (Fig. 4e). Longer parasite survival times increase the probability of indirect epidemiological contact. However, the expected rate of encounter at longer lags approximates the expected rate of encounter under independent movement, so correlations at long lags have only a small modifying effect on the expected FOI. Thus, the increase in FOI due to correlated movement is greatest for parasites with short survival times.

The FOI in general increased as parasites persisted longer in the environment. In contrast, the effect of contact distance varied depending on interaction strength. For pairs with low interaction strength there was no noticeable effect of increasing the threshold contact distance (Fig. 4c). However, for similar trajectories (interaction > 0.9), FOI increased between two and five-fold as contact distance increased, while for identical trajectories (interaction $= 1$) FOI decreased. In our simulation experiments, longer threshold distances translate to larger grid cells, which would decrease FOI as the risk gets diluted in a larger area. The increase in FOI observed therefore responds to the correlation term. Increasing the contact distance increases the probability of finding two individuals in the same cell, and would therefore increase the relative contribution of correlation most for trajectories that are already close in space and time (Fig. 4f), while it would have no effect for trajectories that are far from each other. For identical trajectories, however, grouping observations into larger cells imply fewer cells where correlation is impacting the FOI, and can thus reduce the contribution of correlation and the overall FOI.

Empirical example: white-tailed deer

The total potential FOI varied more than six orders of magnitude across pairs of deer. This was partially due to the difference in spatial overlap, which ranged between 0 and 90% (Bhattacharyya coefficient). While higher overlap generally correlated with higher FOIs, we estimated significantly higher values when we accounted for correlation in movement, and the difference was not necessarily related with greater overlap

(Fig. 5). For the pair with the highest spatial overlap, the FOI was more than ten times greater when we accounted for correlation. For other pairs the effect was less extreme but still considerable; ignoring correlation could result in between 5% and 96% underestimation of FOI. We also noted differences in FOI within each pair, due to the order of visits to the same cells. Difference were usually small (¡5%) but in one case one estimate was 45% higher than the other. We only saw strong effects of correlation when we considered the parasite with a faster decay rate. For a parasite like CWD that can persist for very long in the environment, the FOI was virtually identical with or without the correlation term (Fig. 5XX).

These effects at the local and individual scale will affect inferences made about parasite transmission for the population, for example when calculating metrics like R_0. This can be seen when we plot the contact and transmission networks for our five hosts. The cumulative edge weights would be higher in the case of the short-lived parasite, and we would expect faster transmission through the network than under an assumption of independent movement [TODO: Re-work network plots and calculate relative change in R_0 across the networks].

The increase in FOI due to correlation is not uniform across the area of overlap of individual hosts. Given the localized nature of interactions, the changes in overall FOI are caused by increases at particular cells. Consequently, the estimated FOI is heterogeneous across the landscape.

Discussion

We have developed a new approach for inferring epidemiological dynamics from spatially and temporally explicit data that should facilitate linking these dynamics with underlying environmental factors. Our work generalizes the MoveSTIR framework (Wilber et al., 2022), which translated observed movement and encounter data to the currency of force of infection (FOI). Using a probabilistic perspective, PMoveSTIR provides a direct link between animal movement, utilization distributions (UDs), and epidemiological dynamics, giving a view of FOI across the landscape. UDs are a useful bridge between movement and transmission processes, and we believe their widespread use and intuitive interpretation makes our approach straightforward to apply. Since our framework is explicitly defined in terms of epidemiological processes, we put significant emphasis on temporal dynamics relevant for transmission, such as the rate of contact—direct and indirect—among individuals, the rate of parasite shedding in the environment, and parasite survival in the environment. This framing sets our method apart from recent developments for inferring contact among individuals, which have focused on direct encounters, often assuming independence in movement among hosts (Noonan et al., 2021; Das et al., 2023). While this assumption is convenient and could be sufficient to infer the risk of transmission in some cases, we have shown that it could lead to significant underestimation of

transmission risk, with consequences for inferred disease spread across the population. Our results provide clear expectations for what has been previously observed empirically but largely ignored in movement and disease models – correlation in movement can reshape epidemiological landscapes, leading to hotspots of transmission whose magnitude and location are not necessarily predictable from models of joint space use.

Our results show that correlation in movement and synchronicity can be particularly critical aspects of transmission for faster-paced parasites, i.e. parasites with short environmental persistence and transmission driven by short term contacts (cf. Dougherty et al., 2018; Manlove et al., 2022), such as canine distemper virus, rabies, *Mycoplasma ovipneumoniae*, or SARS-COV-2 (SCV2). SCV2 is of particular interest because recent studies have shown that it can infect a wide-range of wildlife hosts, including white-tailed deer (Palmer et al., 2021; Hale et al., 2022). There is also evidence that white-tailed deer can transmit SCV2 between each other in controlled experiments and in the wild (Martins et al., 2022; Hale et al., 2022), leading to the question of whether SCV2 can successfully invade, spread, and persist in deer populations. Contact is a fundamental component of disease dynamics and our results clearly show that for faster-paced, directly transmitted pathogens like SCV2, the details of fine-scale host movements, beyond joint habitat use, matter greatly for quantifying and predicting invasion, spread, and persistence.

Correlations in space use that are not accounted for by utilization distributions typically reflect social interactions. There are multiple scenarios where strong social interactions can lead to high spatio-temporal overlap: animals moving in groups, parents traveling with their offspring, or mates temporally moving together (Yang et al., 2021) [other citations needed]. This was the case for the deer movements used in this study; the two deer that had the greatest home range overlap, and the highest potential FOI, were does and almost certainly part of the same social group. White-tailed deer female groups have high social affinity during gestation and rut, with groups becoming less cohesive or dissolving entirely during fawning (Koen et al., 2017) [Better citations here...cite deer management book]. Within these groups, pairs of deer have substantially higher contact rates than pairs with equivalent habitat overlap but that are not in the same social group (Schauber et al., 2007; Kjær et al., 2008; Schauber et al., 2015; Grear et al., 2010). Despite similar degrees of habitat overlap as other pairs, the potential force of infection felt between the two focal deer was over 10 times greater than for other pairs. Importantly, 91% of the total FOI for a hypothetical directly transmitted pathogen like SCV2 would be missed if we only considered a joint utilization distribution between these two individuals. While the importance of social interactions on contact rates has been documented previously in white-tailed deer (Grear et al., 2010; Schauber et al., 2015), PMoveSTIR allows us to directly quantify the contribution of these social interactions to the force of infection and move from qualitative conclusions about the importance of social interactions for disease dynamics to movement-informed quantitative models of disease invasion.

In practice, significant correlations that affect FOI beyond the overlap in UDs could also arise from fine-scale temporal patterns of resource use that are not related to social interactions. For example, consider two individuals that move more or less independently but visit a highly localized resource briefly, but at similar times each day (e.g., visiting a watering hole at similar times every day VanderWaal et al., 2017). The overlap of stationary utilization distributions would likely not reflect this area as an area of high contact and transmission risk, primarily because of a mismatch between the long-term use perspective of a UD compared to interactions that are occurring at a fine temporal scale at the localized resource. This interaction would instead be reflected in the correlation term of equation 7 and could greatly affect the estimated FOI. Alternatively, considering temporally varying UDs (i.e. the top right corner in Fig. 1), where the joint probability of use would likely capture both spatial and temporal associations, would reduce the relative importance of spatial-temporal correlations that were not directly related to social interactions. However, non-parametrically estimating transient UDs (e.g., using AKDEs) at fine temporal scales with limited data points is not often feasible. Thus, we expect that epidemiologically important spatial correlations in movement will often be statistically captured by the correlation term of PMoveSTIR, even when they are not directly a result of social interactions.

Currently, our framework relies exclusively on the observed presence/absence data for each cell to estimate these correlations, unlike the spatial overlap estimated using the utilization distribution. Thus, correlation—and by extension FOI—estimates are highly dependent on the data available, which can influence both the values estimated and the location of transmission hotspots. In our simulations the environment is uniform, so the location of cells with meaningful correlations is basically random. Simulating movement for longer provides a more comprehensive view of the correlation surface, which is expected to be uniform and to relate that to the expected probabilities of encounter. There is, however, no evident relationship between the probabilities of use and the estimated local correlation. This is not possible with the empirical data, the data length is what it is. More importantly, the environmental surface is not uniform as in the simulations. I would propose that studying how environment predicts correlation is an important research direction for transmission, as we need to understand the expected correlation between individuals. Methods to estimate the expected correlation, based on social factors or local environmental factors are necessary to obtain a more accurate estimation of the expected FOI.

While spatial correlations in movement can play a sizable role in transmission for fast-paced pathogens, we found that ignoring these interactions may only have marginal effects on transmission for parasites with longer persistence times, like chronic wasting disease and anthrax. Rather, knowing about joint space use is largely sufficient for understanding local transmission risk. Interestingly, empirical transmission patterns of CWD in white-tailed deer populations only partially support this finding, as increased genetic relatedness among

white-tailed deer (i.e., a proxy for social connectedness) increased the probability of CWD infection beyond shared space use (Grear et al., 2010). Given the complex relationship between animal movements and time-lagged correlations in movement (Fig. S1), there are clearly scenarios where correlations in movements and direct contacts still can disproportionately affect transmission risk even for pathogens with long persistence in the environment. The theory we develop here provides a clear, quantitative guide to assess when fine-scale and temporally synchronous movement data is necessary for capturing disease dynamics and when coarser scale, asynchronous movement data focused strictly on UD estimation can be sufficient.

By linking observed movement data and inferred contact with underlying environmental factors, a broad goal of PMoveSTIR is to facilitate the creation of an epidemiological risk landscape that is independent of geographical location, which may enable out-of-sample prediction of transmission risk in novel landscapes (Manlove et al., 2022). Understanding these associations could allow us to forecast future disease dynamics in the study population, project population-wide disease spread as information on more individuals becomes available, or even quantify transmission risk for other populations in similar environments. Previous studies have created system-specific models that make this link, for example using step selection functions with environmental covariates as predictors of daily probabilities of use, and using these probabilities to simulate local disease dynamics (Merkle et al., 2018). Our model provides a generalizable theoretical foundation to perform this type of analysis across different host-parasite systems, and it can be integrated with any method for estimating utilization distributions (Signer et al., 2017; Merkle et al., 2018; Michelot et al., 2020; Potts and Börger, 2023). In addition to covariates that define movement, PMoveSTIR can also incorporate spatially and temporally heterogeneous epidemiological parameters, for example parasite survival rates that vary between habitat types and seasons (Daversa et al., 2017), or spatially localized shedding (Weinstein et al., 2018).

Predicting epidemiological landscapes from host movements relies on the key assumption that environmental characteristics strongly influence movement and space use. While there is a growing number of methods that quantify the effect of environmental characteristics on movement and habitat use (reviewed in Hooten et al., 2017), there has been much less work exploring how (and if) environment affects and predicts correlation and synchrony among hosts [but see citations]. An essential next-step for building epidemiological landscapes will be predictive models of spatio-temporal correlation among individuals. This is an open challenge, though recent progress in predicting the dynamics of group formation will likely be key (e.g. Brandell et al., 2021). Our analyses emphasize the importance of this next step by showing that correlations at a local (cell) scale can create a vastly more heterogeneous transmission landscape, where adjacent cells could have widely different risks of infection. Moreover, correlations can lead to localized transmission hotspots that are not necessarily predictable from joint space use [e.g., Yang et al. in press], and may contribute to the

growing empirical recognition that fine-scale, localized transmission hotspots are present in many empirical host-parasite systems (Albery et al., 2021). Whether these localized transmission hotspots are predictable *a priori* remains to be seen, but ignoring predictors of correlated movements can make the task orders of magnitude more difficult for some pathogens.

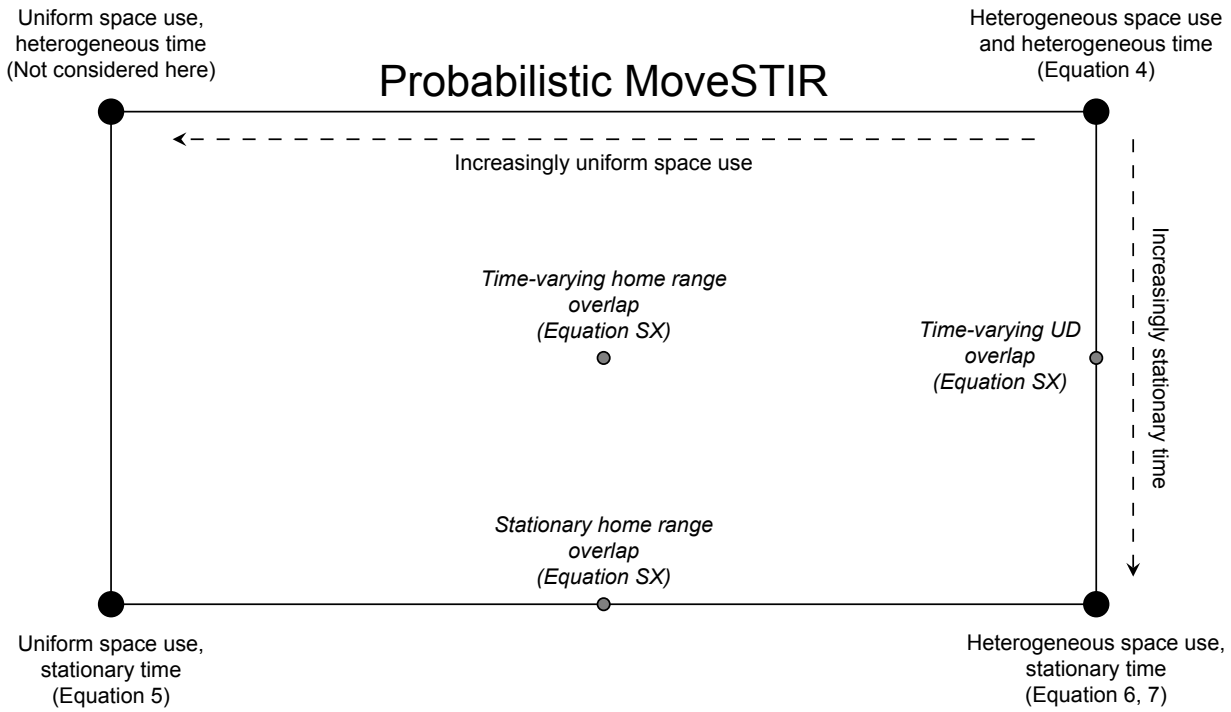

Figure 1: Conceptual figure describing the model developed in this manuscript: probabilistic movement-driven modeling of spatio-temporal infection risk. PMoveSTIR can be thought of as square where the dimensions represent heterogeneity in space and time. The upper right-hand corner has the most general case: heterogeneous space use by hosts, and movement dynamics that are not statistically stationary. As space becomes increasingly uniform or movement becomes more statistically stationary, PMoveSTIR reduces to the upper-left hand corner or the lower-right hand corner, respectively. We primarily focus on the lower-right hand corner in this manuscript. When space use is uniform and movement is statistically stationary, we are in the lower-left hand corner, where we recover mass action transmission as a special case (assuming host movements are uncorrelated).

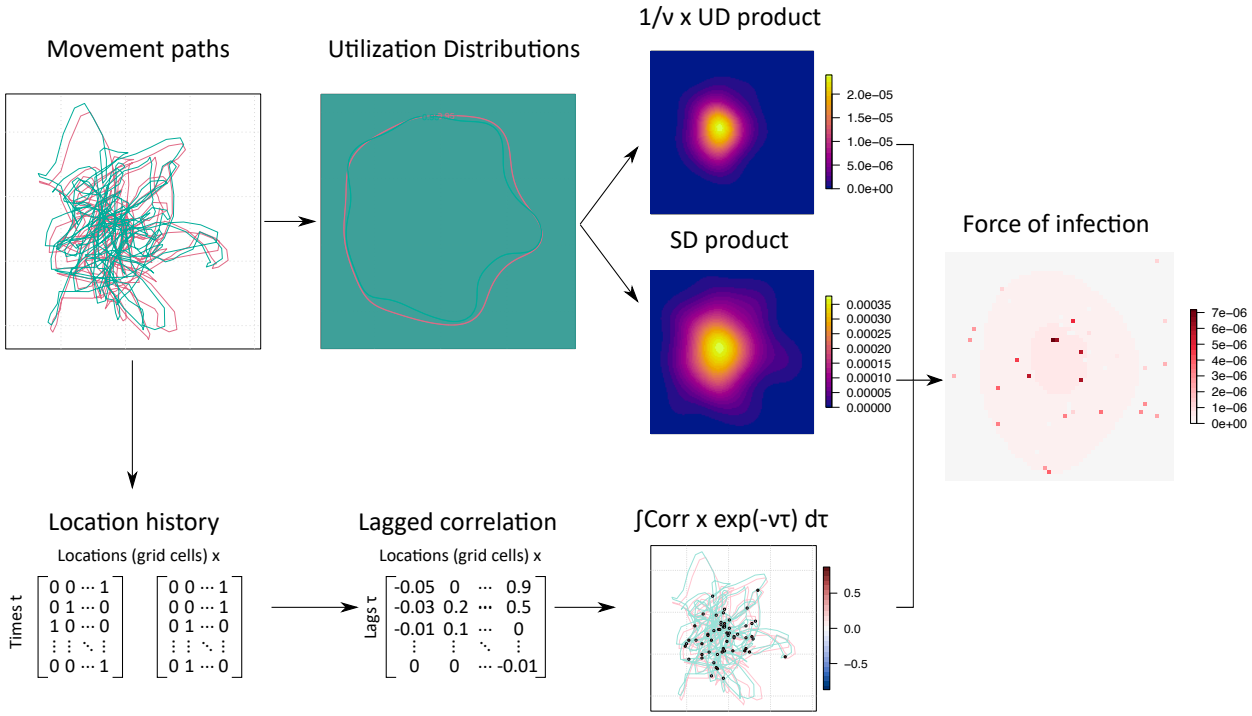

Figure 2: Flow diagram for calculating spatial force of infection (FOI) from movement data using PMoveSTIR. Starting from position data, we estimate individual utilization distributions, and use them to estimate the product of the UDs and their SDs. Parallely, individual position histories are used to estimate the pairwise temporal cross-correlation in space use at each cell. All three elements are combined and scaled by epidemiological parameters to obtain a spatially explicit, pairwise, directional FOI.

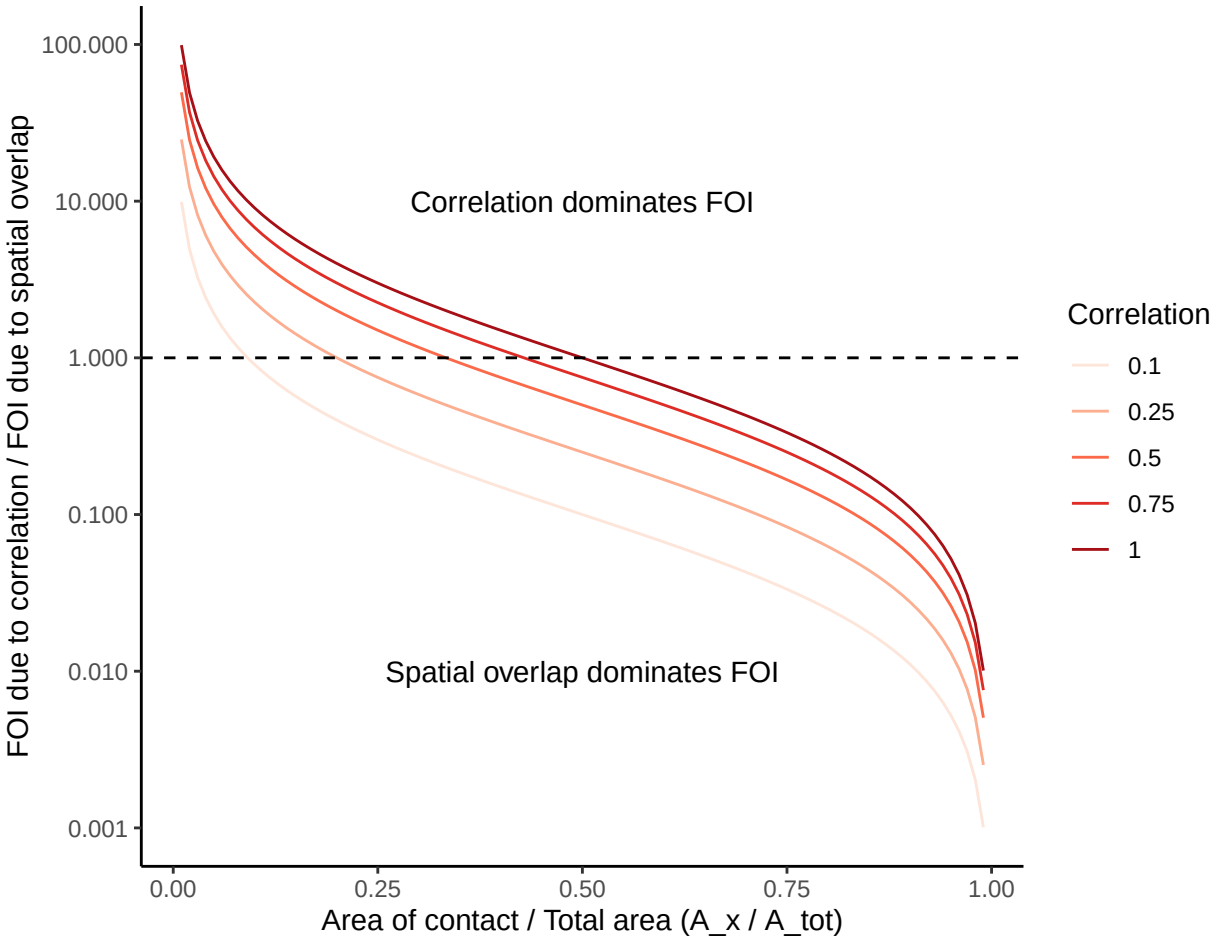

Figure 3: Relationship between the relative contribution of correlation in movement and spatial to pairwise force of infection (FOI) and the relative area of contact. This analytical relationship is derived in equation 9 assuming direct contact. When the relative area of contact is small relative to the total area over which animals can move (e.g., $< 10\%$), even weakly correlated movements can significantly increase force of infection relative to spatial overlap.

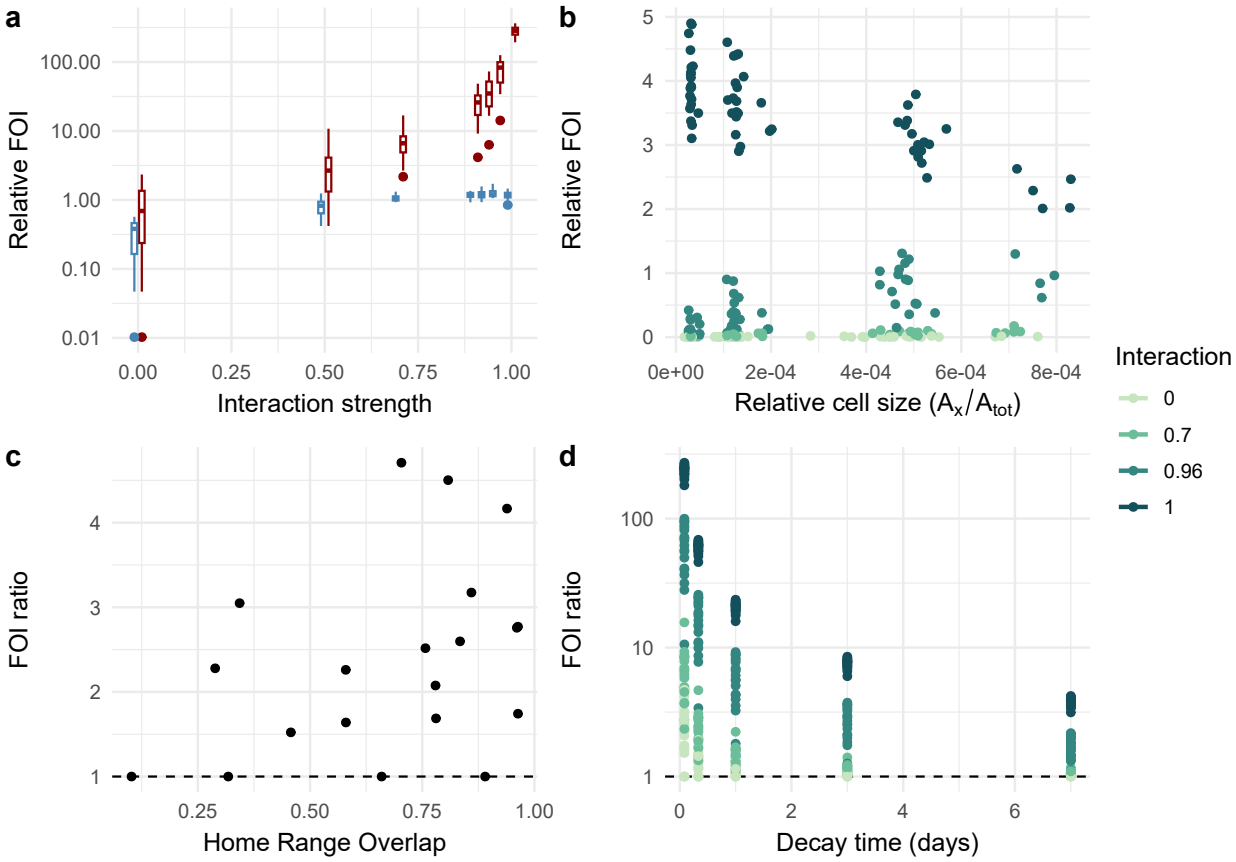

Figure 4: Analysis of simulated movement data show how the force of infection (FOI) varies depending on strength of attraction between individuals and epidemiological parameters such as the decay rate and threshold distance that defines a contact, as well as data availability. **a)** FOI generally increases as a function of attraction strength, but the estimated values are greater when correlation is considered (red boxplots) than when only spatial overlap is considered (blue); **b)** The estimated FOI as a function of home range overlap (as measured by the Bhattacharyya coefficient) shows how correlation can have an apparent effect even for animals that move independently; **c)** Longer epidemiological contact distances can increase, or have no effect on the estimated FOI, depending on the interaction strength; **d)** The contribution of correlation to the overall FOI decreased with longer decay times; **e)** The FOI ratio increases with longer time series as correlation information becomes available for a larger proportion of the space used. A FOI ratio greater than one indicates that correlated movement is increasing FOI relative to spatial overlap and a ratio less than one indicates that correlated movement is decreasing the FOI. In c-e, darker shades indicate stronger attraction between individuals.

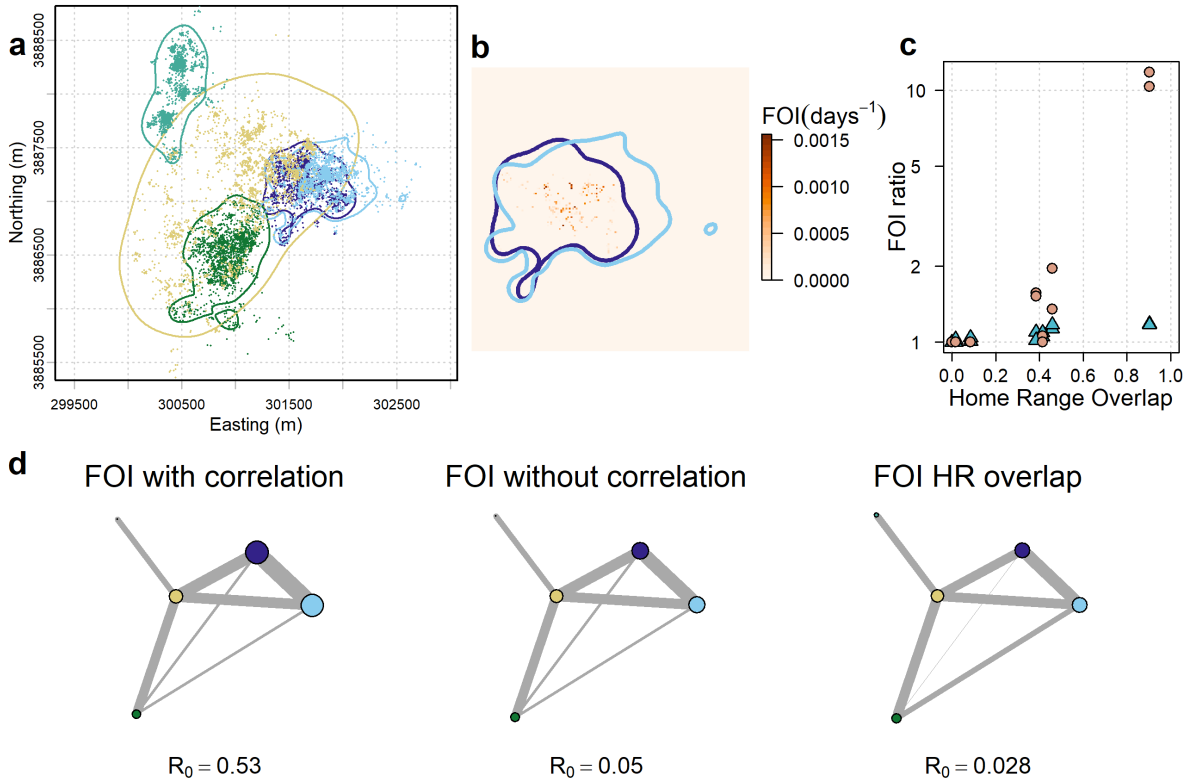

Figure 5: Application of the PMoveSTIR framework to movements of white-tailed deer in TN, USA. a) Home ranges of five individuals with different degrees of overlap. The points show the GPS locations, and the lines are the boundaries of the home ranges, estimated as the region that contains 95% of the utilization distribution density. b) Detail of the home ranges of the two individuals that overlapped the most. The color surface shows the estimated FOI, highlighting how accounting for temporal correlation creates a heterogeneous surface of disease transmission risk with distinct hotspots. c) The ratio of FOI values calculated with versus without correlation shows increased relevance of correlation with higher home range overlap. This effect is greater for parasites with short environmental persistence like SARS-CoV-2 (orange dots) than for parasites with long persistence like CWD (blue triangles). d) Transmission networks created with the PMoveSTIR framework including correlation (left), without correlation (middle), and using the home range overlap (right). The size of the nodes represents the cumulative FOI experienced by each individual, and the width of the edges represents the pairwise FOI. We show only one direction here, but values were similar in both directions within a pair. Sizes and widths have the same scale in all three networks

References

G. F. Albery, A. R. Sweeny, D. J. Becker, and S. Bansal. Fine-scale spatial patterns of wildlife disease are common and understudied. *Functional Ecology*, 36(October 2020):214–225, 2021. ISSN 13652435. doi: 10.1111/1365-2435.13942.

J. M. Alston, C. H. Fleming, M. J. Noonan, M. A. Tucker, I. Silva, C. Folta, T. S. Akre, A. H. Ali, J. L. Belant, D. Beyer, N. Blaum, K. Böhning-Gaese, R. C. de Paula, J. Dekker, J. Drescher-Lehman, N. Farwig, C. Fichtel, C. Fischer, A. T. Ford5, R. Janssen, F. Jeltsch, P. M. Kappeler, S. D. LaPoint, A. C. Markham, E. P. Medic, R. G. Morato, R. Nathan, K. A. Olson, B. D. Patterson, T. R. Petroelje, E. E. Ramalho, S. Rösner, L. G. O. Santos, D. G. Schabo, N. Selva, A. Sergiel, O. Spiegel, W. Ullmann, F. Zieba, T. Zwiacz-Kozica, G. Wittemyer, W. F. Fagan, T. Müller, and J. M. Calabrese. Clarifying space use concepts in ecology : range vs . occurrence distributions (preprint). *bioRxiv preprint*, page 2022.09.29.509951, 2022. URL `https://www.biorxiv.org/content/10.1101/2022.09.29.509951v1%0Ahttps://www.biorxiv.org/content/10.1101/2022.09.29.509951v1.abstract%0Ahttps://doi.org/10.1101/2022.09.29.509951`.

E. E. Brandell, A. P. Dobson, P. J. Hudson, P. C. Cross, and D. W. Smith. A metapopulation model of social group dynamics and disease applied to Yellowstone wolves. *Proceedings of the National Academy of Science*, 118(March):e2020023118, 2021. doi: 10.1073/pnas.2020023118.

J. M. Calabrese, C. H. Fleming, and E. Gurarie. ctmm: an r package for analyzing animal relocation data as a continuous-time stochastic process. *Methods in Ecology and Evolution*, 7(9):1124–1132, sep 2016. ISSN 2041-210X. doi: 10.1111/2041-210X.12559. URL `https://besjournals.onlinelibrary.wiley.com/doi/10.1111/2041-210X.12559https://onlinelibrary.wiley.com/doi/10.1111/2041-210X.12559`.

M. H. Cortez and M. A. a. Duffy. The Context-Dependent Effects of Host Competence, Competition, and Pathogen Transmission Mode on Disease Prevalence. *The American Naturalist*, 198(2):179–194, 2021. ISSN 0003-0147. doi: 10.1086/715110.

D. Das, V. M. Kenkre, R. Nathan, and L. Giuggioli. Misconceptions about quantifying animal encounter and interaction processes. *Frontiers in Ecology and Evolution*, 11:1230890, 2023. doi: 10.3389/fevo.2023.1230890.

D. R. Daversa, A. Fenton, A. I. Dell, T. W. Garner, and A. Manica. Infections on the move: How transient phases of host movement influence disease spread. *Proceedings of the Royal Society B: Biological Sciences*, 284(1869), 2017. ISSN 14712954. doi: 10.1098/rspb.2017.1807.

R. T. Dean and W. T. M. Dunsmuir. Dangers and uses of cross-correlation in analyzing time series in perception, performance, movement, and neuroscience: The importance of constructing transfer function autoregressive models. *Behavior Research Methods*, 48(2):783–802, jun 2016. ISSN 1554-3528. doi: 10.3758/s13428-015-0611-2. URL http://link.springer.com/10.3758/s13428-015-0611-2.

E. R. Dougherty, D. P. Seidel, C. J. Carlson, O. Spiegel, and W. M. Getz. Going through the motions: Incorporating movement analyses into disease research. *Ecology Letters*, pages 588–604, 2018. ISSN 14610248. doi: 10.1111/ele.12917.

E. R. Dougherty, D. P. Seidel, J. K. Blackburn, W. C. Turner, and W. M. Getz. A framework for integrating inferred movement behavior into disease risk models. *Movement Ecology*, 10(1), dec 2022. ISSN 20513933. doi: 10.1186/S40462-022-00331-8.

J. A. Drewe, N. Weber, S. P. Carter, S. Bearhop, X. A. Harrison, S. R. Dall, R. A. McDonald, and R. J. Delahay. Performance of proximity loggers in recording intra- and inter-species interactions: A laboratory and field-based validation study. *PLoS ONE*, 7(6):e39068, 2012. ISSN 19326203. doi: 10.1371/journal.pone.0039068.

C. H. Fleming, J. M. Calabrese, T. Mueller, K. A. Olson, P. Leimgruber, and W. F. Fagan. Non-Markovian maximum likelihood estimation of autocorrelated movement processes. *Methods in Ecology and Evolution*, 5(5):462–472, may 2014. ISSN 2041210X. doi: 10.1111/2041-210X.12176. URL https://besjournals.onlinelibrary.wiley.com/doi/10.1111/2041-210X.12176https://onlinelibrary.wiley.com/doi/10.1111/2041-210X.12176.

S. S. Godfrey. Networks and the ecology of parasite transmission: A framework for wildlife parasitology. *International journal for parasitology. Parasites and wildlife*, 2:235–45, dec 2013. ISSN 2213-2244. doi: 10.1016/j.ijppaw.2013.09.001.

S. S. Godfrey, J. A. Moore, N. J. Nelson, and C. M. Bull. Social network structure and parasite infection patterns in a territorial reptile, the tuatara (Sphenodon punctatus). *International Journal for Parasitology*, 40(13):1575–1585, 2010. ISSN 0020-7519. doi: https://doi.org/10.1016/j.ijpara.2010.06.002. URL https://www.sciencedirect.com/science/article/pii/S002075191000247X.

D. A. Grear, M. D. Samuel, K. T. Scribner, B. V. Weckworth, and J. A. Langenberg. Influence of genetic relatedness and spatial proximity on chronic wasting disease infection among female white-tailed deer. *Journal of Applied Ecology*, 47(3):532–540, 2010. ISSN 00218901. doi: 10.1111/j.1365-2664.2010.01813.x.

G. Grimmett and D. Stirzaker. *Probability and random processes* . Oxford University Press, Oxford ;, 3rd ed. edition, 2001. ISBN 0198572239.

E. Gurarie and O. Ovaskainen. Towards a general formalization of encounter rates in ecology. *Theoretical Ecology*, 6(2):189–202, 2013. ISSN 18741746. doi: 10.1007/s12080-012-0170-4.

V. L. Hale, P. M. Dennis, D. S. McBride, J. M. Nolting, C. Madden, D. Huey, M. Ehrlich, J. Grieser, J. Winston, D. Lombardi, S. Gibson, L. Saif, M. L. Killian, K. Lantz, R. M. Tell, M. Torchetti, S. Robbe-Austerman, M. I. Nelson, S. A. Faith, and A. S. Bowman. SARS-CoV-2 infection in free-ranging white-tailed deer. *Nature*, 602(7897):481–486, 2022. ISSN 14764687. doi: 10.1038/s41586-021-04353-x.

M. B. Hooten, D. S. Johnson, B. T. McClintock, and J. M. Morales. *Animal Movement: Statistical Models for Telemetry Data*. CRC Press, New York, USA, 2017.

L. J. Kjær, E. M. Schauber, and C. K. Nielsen. Spatial and Temporal Analysis of Contact Rates in Female White-Tailed Deer. *Journal of Wildlife Management*, 72(8):1819–1825, 2008. ISSN 0022-541X. doi: 10.2193/2007-489.

E. L. Koen, M. I. Tosa, C. K. Nielsen, and E. M. Schauber. Does landscape connectivity shape local and global social network structure in white-tailed deer? *PLoS ONE*, 12(3):1–21, 2017. ISSN 19326203. doi: 10.1371/journal.pone.0173570.

B. Kranstauber, R. Kays, S. D. LaPoint, M. Wikelski, and K. Safi. A dynamic Brownian bridge movement model to estimate utilization distributions for heterogeneous animal movement. *Journal of Animal Ecology*, 81(4):738–746, jul 2012. ISSN 00218790. doi: 10.1111/j.1365-2656.2012.01955.x. URL `https://besjournals.onlinelibrary.wiley.com/doi/10.1111/j.1365-2656.2012.01955.xhttps://onlinelibrary.wiley.com/doi/10.1111/j.1365-2656.2012.01955.x`.

K. Manlove, C. Aiello, P. Sah, B. Cummins, P. J. Hudson, and P. C. Cross. The ecology of movement and behaviour: A saturated tripartite network for describing animal contacts. *Proceedings of the Royal Society B: Biological Sciences*, 285(1887), 2018. ISSN 14712954. doi: 10.1098/rspb.2018.0670.

K. Manlove, M. Wilber, L. White, G. Bastille-Rousseau, A. Yang, M. L. Gilbertson, M. E. Craft, P. C. Cross, G. Wittemyer, and K. M. Pepin. Defining an epidemiological landscape that connects movement ecology to pathogen transmission and pace-of-life. *Ecology Letters*, 25(8):1760–1782, aug 2022. ISSN 14610248. doi: 10.1111/ELE.14032. URL `https://click.endnote.com/viewer?doi=10.1111{%}2Fele.14032{&}token=WzI0NjA5NTUsIjEwLjExMTEvZWxlLjE0MDMyIl0.ZF0my4FtNLVSqDzt46qYttkAfps`.

R. Martinez-Garcia, C. H. Fleming, R. Seppelt, W. F. Fagan, and J. M. Calabrese. How range residency and long-range perception change encounter rates. *Journal of Theoretical Biology*, 498:110267, 2020. ISSN 10958541. doi: 10.1016/j.jtbi.2020.110267. URL https://doi.org/10.1016/j.jtbi.2020.110267.

M. Martins, P. M. Boggiatto, A. Buckley, E. D. Cassmann, S. Falkenberg, L. C. Caserta, M. H. Fernandes, C. Kanipe, K. Lager, M. V. Palmer, and D. G. Diel. From Deer-To-Deer: SARS-CoV-2 is efficiently transmitted and presents broad tissue tropism and replication sites in white-Tailed deer. *PLoS Pathogens*, 18(3):1–26, 2022. ISSN 15537374. doi: 10.1371/journal.ppat.1010197. URL http://dx.doi.org/10.1371/journal.ppat.1010197.

H. McCallum. How should pathogen transmission be modelled? *Trends in Ecology and Evolution*, 16(6): 295–300, jun 2001. ISSN 01695347. doi: 10.1016/S0169-5347(01)02144-9.

J. A. Merkle, P. C. Cross, . Brandon, M. Scurlock, E. K. Cole, A. B. Courtemanch, S. R. Dewey, . Matthew, and J. Kauffman. Linking spring phenology with mechanistic models of host movement to predict disease transmission risk. *J Appl Ecol*, 55:810–819, 2018. doi: 10.1111/1365-2664.13022. URL https://besjournals.onlinelibrary.wiley.com/doi/10.1111/1365-2664.13022.

T. Michelot, P. G. Blackwell, S. Chamaillé-Jammes, and J. Matthiopoulos. Inference in MCMC step selection models. *Biometrics*, 76(2):438–447, jun 2020. ISSN 1541-0420. doi: 10.1111/BIOM.13170. URL https://onlinelibrary.wiley.com/doi/full/10.1111/biom.13170https://onlinelibrary.wiley.com/doi/abs/10.1111/biom.13170https://onlinelibrary.wiley.com/doi/10.1111/biom.13170.

M. J. Noonan, R. Martinez-Garcia, G. H. Davis, M. C. Crofoot, R. Kays, B. T. Hirsch, D. Caillaud, E. Payne, A. Sih, D. L. Sinn, O. Spiegel, W. F. Fagan, C. H. Fleming, and J. M. Calabrese. Estimating encounter location distributions from animal tracking data. *Methods in Ecology and Evolution*, 12(7):1158–1173, 2021. ISSN 2041210X. doi: 10.1111/2041-210X.13597.

M. V. Palmer, M. Martins, S. Falkenberg, A. Buckley, L. C. Caserta, P. K. Mitchell, E. D. Cassmann, A. Rollins, N. C. Zylich, R. W. Renshaw, C. Guarino, B. Wagner, K. Lager, and D. G. Diel. Susceptibility of White-Tailed Deer (Odocoileus virginianus) to SARS-CoV-2. *Journal of Virology*, 95(11), 2021. ISSN 0022-538X. doi: 10.1128/jvi.00083-21.

J. R. Potts and L. Börger. How to scale up from animal movement decisions to spatiotemporal patterns: An approach via step selection. *Journal of Animal Ecology*, 92(1):16–29, jan 2023. ISSN 1365-2656. doi: 10.1111/1365-2656.13832. URL https://onlinelibrary.wiley.com/doi/full/10.1111/

1365-2656.13832https://onlinelibrary.wiley.com/doi/abs/10.1111/1365-2656.13832https://besjournals.onlinelibrary.wiley.com/doi/10.1111/1365-2656.13832.

T. O. Richardson and T. E. Gorochowski. Beyond contact-based transmission networks: the role of spatial coincidence. *Journal of The Royal Society Interface*, 12(111):20150705, sep 2015. ISSN 1742-5689. doi: 10.1098/rsif.2015.0705. URL http://rsif.royalsocietypublishing.org/content/12/111/20150705.abstract.

P. Sah, J. Mann, and S. Bansal. Disease implications of animal social network structure: A synthesis across social systems. *Journal of Animal Ecology*, 87(3):546–558, may 2018. ISSN 0021-8790. doi: https://doi.org/10.1111/1365-2656.12786. URL https://doi.org/10.1111/1365-2656.12786.

S. E. Saunders, S. L. Bartelt-Hunt, and J. C. Bartz. Occurrence, transmission, and zoonotic potential of chronic wasting disease. *Emerging Infectious Diseases*, 18(3):369–376, 2012. ISSN 10806040. doi: 10.3201/eid1803.110685.

H. R. Scharf, M. B. Hooten, D. S. Johnson, and J. W. Durban. Process convolution approaches for modeling interacting trajectories. *Environmetrics*, 29(3), may 2018. ISSN 1099095X. doi: 10.1002/ENV.2487. URL https://click.endnote.com/viewer?doi=10.1002{%}2Fenv.2487{&}token=WzIONjA5NTUsIjEwLjEwMDIvZW52LjIOODciXQ.xe6HpMRvQJju5QhPGiUKaUZXEkc.

E. M. Schauber, D. J. Storm, and C. K. Nielsen. Effects of Joint Space Use and Group Membership on Contact Rates Among White-Tailed Deer. *Journal of Wildlife Management*, 71(1):155–163, 2007. ISSN 0022-541X. doi: 10.2193/2005-546.

E. M. Schauber, C. K. Nielsen, L. J. Kjær, C. W. Anderson, and D. J. Storm. Social affiliation and contact patterns among white-tailed deer in disparate landscapes: Implications for disease transmission. *Journal of Mammalogy*, 96(1):16–28, 2015. ISSN 15451542. doi: 10.1093/jmammal/gyu027.

J. Signer, J. Fieberg, and T. a. Avgar. Estimating utilization distributions from fitted step-selection functions. *Ecosphere*, 8(4):e01771, 2017. ISSN 2150-8925. doi: 10.1002/ecs2.1771. URL http://10.0.3.234/ecs2.1771https://dx.doi.org/10.1002/ecs2.1771https://kp-pdf.s3.amazonaws.com/c83c0cea-1232-4447-9e78-4f565524f03f.pdf?X-Amz-Algorithm=AWS4-HMAC-SHA256{&}X-Amz-Credential=AKIAUROH2NUQSIQZIEG4{%}2F20230601{%}2Fus-east-1{%}2Fs3{%}2Faws4{_}20230601T083908Z{&}X-Amz-Expires=600{&}X-Amz-SignedHeaders=host{&}X-Amz-Signature=3fed727f1a486ca7dad79a1370c73b436aa3e854cde649b9a6a4cd8ce8c3beb4.

Y. Tao, L. Börger, and A. Hastings. Dynamic Range Size Analysis of Territorial Animals: An Optimality Approach. *The American Naturalist*, 188(4):460–474, 2016. ISSN 0003-0147. doi: 10.1086/688257. URL http://10.0.4.62/688257https://dx.doi.org/10.1086/688257.

G. Titcomb, J. N. Mantas, J. Hulke, I. Rodriguez, D. Branch, and H. Young. Water sources aggregate parasites with increasing effects in more arid conditions. *Nature Communications*, 12(1):1–12, 2021. ISSN 20411723. doi: 10.1038/s41467-021-27352-y.

K. VanderWaal, M. Gilbertson, S. Okanga, B. F. Allan, and M. E. Craft. Seasonality and pathogen transmission in pastoral cattle contact networks. *Royal Society Open Science*, 4(12):170808, 2017. ISSN 20545703. doi: 10.1098/rsos.170808.

Q. M. Webber, G. F. Albery, D. R. Farine, N. Pinter-Wollman, N. Sharma, O. Spiegel, E. Vander Wal, and K. Manlove. Behavioural ecology at the spatial–social interface. *Biological Reviews*, 98(3):868–886, jun 2023. ISSN 1469-185X. doi: 10.1111/BRV.12934. URL https://onlinelibrary.wiley.com/doi/full/10.1111/brv.12934https://onlinelibrary.wiley.com/doi/abs/10.1111/brv.12934https://onlinelibrary.wiley.com/doi/10.1111/brv.12934.

S. B. Weinstein, C. W. Moura, J. F. Mendez, and K. D. Lafferty. Fear of feces? Tradeoffs between disease risk and foraging drive animal activity around raccoon latrines. *Oikos*, 127(7):927–934, 2018. ISSN 16000706. doi: 10.1111/oik.04866.

M. Q. Wilber, A. Yang, R. Boughton, K. R. Manlove, R. S. Miller, K. M. Pepin, and G. Wittemyer. A model for leveraging animal movement to understand spatio-temporal disease dynamics. *Ecology Letters*, 25(5):1290–1304, may 2022. ISSN 1461-023X. doi: 10.1111/ele.13986.

K. Winner, M. J. Noonan, C. H. Fleming, K. A. Olson, T. Mueller, D. Sheldon, and J. M. Calabrese. Statistical inference for home range overlap. *Methods in Ecology and Evolution*, 9(7):1679–1691, jul 2018. ISSN 2041210X. doi: 10.1111/2041-210X.13027.

B. J. Worton. Kernel methods for estimating the utilization distribution in home-range studies. *Ecology*, 70 (1):164–168, 1989. doi: https://doi.org/10.2307/1938423. URL https://esajournals.onlinelibrary.wiley.com/doi/abs/10.2307/1938423.

A. Yang, . P. Schlichting, B. Wight, W. M. Anderson, S. M. Chinn, M. Q. Wilber, R. S. Miller, . James, C. Beasley, R. K. Boughton, K. C. Vercauteren, . G. Wittemyer, . Kim, and M. Pepin. Effects of social structure and management on risk of disease establishment in wild pigs. *J Anim Ecol*, 90:820–833, 2021.

710 doi: 10.1111/1365-2656.13412. URL https://besjournals.onlinelibrary.wiley.com/doi/10.1111/
711 1365-2656.13412.

712 A. Yang, M. Q. Wilber, K. R. Manlove, R. S. Miller, R. Boughton, J. Beasley, J. Northrup, K. C. Vercauteren,
713 . George Wittemyer, and . K. Pepin. Deriving spatially explicit direct and indirect interaction networks
714 from animal movement data. *Ecology and Evolution*, 13, 2023. doi: 10.1002/ece3.9774.